# ХІМІЧНА ІНЖЕНЕРІЯ

UDC 621.793.7:546.26-023.847:678.744.3

Oleksandr GONDLIAKH <sup>1</sup>, Illia YANKOVSKYI <sup>1\*</sup>, Sergiy ANTONYUK <sup>2</sup>

<sup>1</sup> National Technical University of Ukraine "Igor Sikorsky Kyiv Polytechnic Institute", Kyiv, Ukraine 

<sup>2</sup> University of Kaiserslautern-Landau, Kaiserslautern, Germany

# FEATURES OF CARBON NANOTUBES DEPOSITION ON A POLYMER SUBSTRATE BY COLD GAS-DYNAMIC SPRAY TECHNIQUE

Cold gas-dynamic spraying of carbon nanotubes onto polymer substrates is a promising technique for the formation of functional coatings. However, the process of particle deposition on polymer substrates remains insufficiently studied. In this study, a numerical model was developed to analyze the mechanisms of contact interaction between nanotubes and a polyetheretherketone substrate during deposition. The effect of particle velocity on plastic deformation, local heating, and the conditions for nanotube bonding to the polymer substrate has been investigated. The obtained results show the existence of a threshold velocity at which effective mechanical bonding occurs. The conditions for local temperature rise in the substrate, which may promote the formation of a stable nanocomposite coating, have also been analyzed. The proposed model enables the prediction of optimal deposition parameters to ensure high efficiency of nanotube deposition.

Keywords: cold gas-dynamic spraying, carbon nanotubes, polyetheretherketone, finite element method

### DOI: 10.20535/2617-9741.3.2025.340369

\* Corresponding author: il.yankovskyi@gmail.com Received 14 May 2025; Accepted 05 June 2025

**Statement of the problem.** Over the past decades, the processes of functional coating formation have been actively developed and thoroughly studied. Special attention has been given to techniques for particle deposition onto various substrates with the aim of creating highly efficient and strong joints. One of the most promising approaches in this field is the method of cold gas-dynamic spraying (CGDS), a process in which particles are accelerated to supersonic velocities by a gas flow and deposit onto the surface without melting, due to their kinetic energy.

Despite the significant number of studies on cold spray technologies, most of them have focused on "metal-metal" systems, in which both the adhesion mechanisms and the nature of particle-substrate interactions have been well investigated. Nevertheless, with technological advancements, there is a growing interest in applying CGDS for the deposition of carbon nanotubes (CNT) onto polymer substrates, as this may pave the way for the creation of new, lightweight, strong, and functional nanomodified coatings.

One of the key aspects determining the efficiency of CNT deposition by the CGDS method is the critical velocity, the minimum velocity at which nanotubes can be reliably fixed on the surface of a polymer substrate. Determining the adhesion mechanisms and critical velocity values during contact interaction of CNTs with polymer materials is a non-trivial task due to the specifics of the processes of their micro- and nanoscale contact interactions, as well as the limitations of obtaining experimental data due to the short duration of contact during high-speed impacts.

Due to the difficulties in experimentally monitoring high-velocity deposition processes, numerical simulation has become an important tool for conducting such studies.

Analysis of previous studies. Cold spraying (or simply cold spraying) is an innovative coating technology developed in the mid-1980s during model studies of two-phase supersonic flow [1]. However, this method has only recently gained popularity in the aerospace and other industries as a method for repair and restoration of metal parts [2].

Unlike the cold spraying method, the classic thermal spraying process involves heating the particles to temperatures often exceeding their melting point. Due to the high operating temperatures during thermal spraying, pore formation, increased oxide content and the occurrence of a residual stress field are inevitable. These defects can significantly worsen the mechanical, electrical and thermal properties of the coatings [3].

In contrast, deposition by the CGDS method is conducted at significantly lower gas flow temperatures (ranging from -100 to +100 °C), which eliminates the problems inherent in classical thermal spraying [3].

9

<sup>©</sup> The Author(s) 2025. Published by Igor Sikorsky Kyiv Polytechnic Institute. This is an Open Access article distributed under the terms of the license CC BY 4.0 (https://creativecommons.org/licenses/by/4.0/), which permits re-use, distribution, and reproduction in any medium, provided the original work is properly cited.

The coating formation process consists of several key stages. Initially, particles are accelerated to supersonic velocities in a gas flow while passing through a de Laval nozzle. Then, they impact the substrate, where zones of plastic deformation are momentarily formed in the contact area. As a result, a local adhesion zone is created due to the high impact velocity and localized heating. If the particle velocity is below the critical value, the particle fails to form a strong bond and may either cause minor damage to the substrate or be swept away by the gas flow. When the critical velocity is exceeded, the particles effectively adhere to the substrate, forming a dense coating layer.

Studies conducted in the early stages of cold spray deposition process research demonstrated the critical role of particle impact velocity on the substrate surface [4]. However, the binding mechanism depends not only on the velocity but also on several additional factors including impact angle [5], substrate surface temperature [6], working gas properties [7], and deposited material properties [8].

In the case of cold gas-dynamic spraying, the bond between the particle and the substrate in metal-to-metal systems occurs due to adiabatic shear instability [9] at the particle-substrate interface.

When particles impact, localized regions with elevated temperatures and intense plastic deformation of both the particle and the substrate are formed. When critical parameters are reached, the material in the contact zone undergoes significant softening, which facilitates the formation of microwelded joints between the particle and the substrate. An important condition for effective adhesion is the formation of a thin stream of displaced particle material surrounding the contact zone, which additionally enhances mechanical adhesion [9].

In the study [10], 3D numerical simulations of high-speed impacts of copper and aluminum particles during cold spraying were performed using the finite element method in the ABAQUS/Explicit software in the Lagrangian coordinate system. The main focus was on the analysis of plastic deformation of particles, determination of the critical deposition velocity and investigation of the effects of material damage.

The results demonstrated that at velocities below 250 m/s, plastic deformation was insufficient to achieve bonding with the substrate. In the velocity range of 300 to 600 m/s, microwelded joints were formed, while velocities above 600 m/s led to overheating and microcrack formation. To minimize FE-mesh distortions, the Arbitrary Lagrangian-Eulerian (ALE) method was tested, but it caused abnormal elongation of the particles.

The combination of the Lagrangian approach and the Johnson-Cook damage model proved to be more effective, as it allowed for efficient modeling of the deformation accumulation processes and the evolution of the development of material damage zones. The critical deposition velocities were determined to be approximately 300 m/s for copper powder and approximately 350 m/s for aluminum. These values are consistent with experimental data and confirm the effectiveness of the Lagrangian method in combination with the damage model for modeling the cold spraying process.

Unlike in metals, where adiabatic shear instability plays a key role in forming strong bonds between particles and substrates, this phenomenon has a much smaller effect in polymer materials due to their fundamentally different chemical nature. Therefore, for polymers, mechanical interlocking is considered the primary bonding mechanism [11].

The efficiency of adhesion and coating formation on polymer substrates can be reduced due to their low stiffness and further softening caused by heat generated during particle impacts. This is an important factor to consider when simulating the cold spray deposition process on polymers [12].

In [13], the authors presented a simulation of copper particle deposition on a polyetheretherketone (PEEK) substrate. They performed parallel simulations using two different approaches: adiabatic analysis and coupled thermostructural analysis. Comparison of the results did not reveal any significant differences in the deformation patterns and crater geometry formed by particle impacts on the polymer substrate.

Because the study focused primarily on the mechanical behavior of the material under plastic deformation, the authors concluded that adiabatic heating analysis coupled with damping boundary conditions provides an effective means to describe the mechanical coupling between metal particles and polymer substrates. However, coupled thermostructural analysis offers a more realistic temperature.

The results confirmed limited surface melting of the polymer inside the crater. As particle velocity increased, a larger volume of polymer melted due to greater heat dissipation. Although the melted region remained small and shallow relative to the crater size, the presence of molten polymer was found to enhance mechanical adhesion by acting like an adhesive that slows down and secures the particle within the polymer matrix.

Despite the high popularity of CGDS, as evidenced by numerous studies on adhesion mechanisms and the interaction of metal particles with metal substrates or polymers, the use of composite materials, particularly those combining carbon nanotubes (CNT) with metals or polymers, remains insufficiently explored. Existing studies mainly focus on conventional metal powders and their deposition mechanisms, while the influence of composite particle characteristics (CNT/metal and CNT/polymer) on the spraying process, deposition efficiency, and coating

morphology has been investigated only fragmentarily. CNT-based composites exhibit unique properties, such as high mechanical strength, electrical conductivity, and thermal stability, making them promising candidates for the development of functional coatings. However, their complex structure and specific behavior during deposition introduce additional challenges that require detailed analysis and optimization of the process parameters.

In [14, 15], the authors reported successful deposition of a nanomodified polymer consisting of carbon nanotubes and polyethylene (NMPE) on a polypropylene (PP) substrate. It was found that during the deposition process, NMPE particles were briefly heated by the working gas. Since the gas temperature exceeded the melting point of PE ( $\approx$ 373 K) but remained below its thermal decomposition temperature ( $\approx$ 550 K), partial melting of the surface layer of NMPE particles occurred, leading to their coalescence upon contact with the PP substrate. This effect was confirmed by the altered particle shapes observed in SEM images.

During deposition, the molten NMPE particles rapidly solidified due to efficient heat exchange with the substrate. This mechanism differs from the formation of metallic coatings via cold spraying, as partial softening without complete melting plays a crucial role in the case of polymer particles. An important outcome is that partial melting of PE promotes the anchoring of CNT on the surface, either by embedding the nanotubes into the molten polymer or leaving them partially exposed.

**Summary.** The analysis of previous studies has shown that cold gas-dynamic spraying is a promising technology that enables the fabrication of coatings without significant heating of materials. The principal bonding mechanism between metal particles and metal substrates is adiabatic shear instability, whereas, for polymer substrates, mechanical bonding predominates. Regardless of the material type, the critical velocity of the deposited material plays a key role in successful coating formation. Although the process of coating formation on metals and polymers has been studied in detail, the interaction mechanisms between carbon nanotubes and polymer substrates remain understudied. The available literature primarily focuses on the deposition of metals, while the effects of nanofillers on coating formation have not yet received sufficient attention.

The aim of the study. The main objective of this study is to develop a model for numerical simulation of contact interaction processes during supersonic deposition of carbon nanotubes on polymer substrates using cold gas-dynamic spraying.

**Presentation of the main materials of calculations.** Nanotubes are deposited on a substrate by accelerating them to high speeds and then contacting the substrate material. This process involves complex physical interactions, including momentum transfer, plastic deformation of the substrate, local temperature increase, and the emergence and development of damage zones.

At the initial stage, the nanotube moves toward the substrate with some initial velocity, which determines its kinetic energy and penetration depth. Upon impact, the nanotube slows down sharply, transferring its kinetic energy to the substrate material. As a result, local adiabatic compression occurs, accompanied by an instantaneous increase in pressure and temperature. The impact generates stress waves that propagate from the point of contact and can cause plastic deformation of the substrate. In the contact zone, there is a sharp increase in temperature due to the dissipation of mechanical energy and accumulation of damage.

Part of the impact energy is expended in the formation of a penetration crater, causing outward displacement of the substrate material. If the temperature rise is significant, partial softening or even melting of the substrate may occur. After the initial penetration, the nanotube may either be embedded in the substrate material or rebound. If the zone of plastic deformation is sufficiently developed and the impact velocity is optimal, the substrate material closes around the nanotube, anchoring it within the structure. Conversely, if the impact energy is insufficient or the substrate is too rigid, the nanotube rebounds. This occurs due to the elastic properties of the polymer material and the partial restitution of the initial kinetic energy from the polymer to the nanotube.

Numerical modeling of cold spray deposition of carbon nanotubes (CNTs) on a polyetheretherketone (PEEK) substrate was performed using the finite element method and ABAQUS/Explicit software.

As part of the study, a three-dimensional model was developed to enable monitoring of the behavior of CNT during high-velocity impacts with a polymer surface (Fig. 1).

The explicit time integration scheme has been used, as it is best suited for simulating non-stationary dynamic processes, strains, and fractures arising during high-velocity impacts. To improve the accuracy of thermal process modeling following the impact, a dynamic coupled thermo-mechanical analysis was performed. The discretization of the CNT and the substrate geometries (Fig. 2) was carried out using 345 and 249900 volume eight-node trilinear elements with displacement and temperature degrees of freedom, reduced integration, and shear instability control (C3D8RT). In areas of intensive strain, a refined mesh was applied to achieve higher accuracy while reducing computational costs. Geometric nonlinear effects were accounted for throughout the simulation by enabling the

«Nlgeom» option. The contact between the CNT and the substrate was modeled as the «surface-to-surface» contact type using the «penalty contact method» for mechanical interaction, with «finite sliding» allowed.

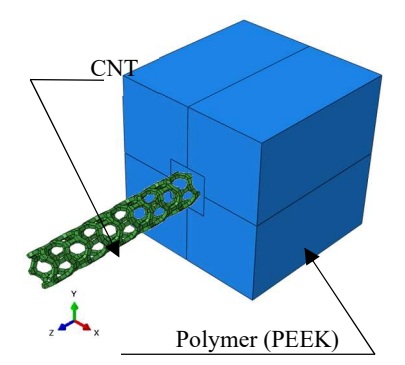


Fig. 1 – Computational scheme of CNT and PEEK polymer substrate

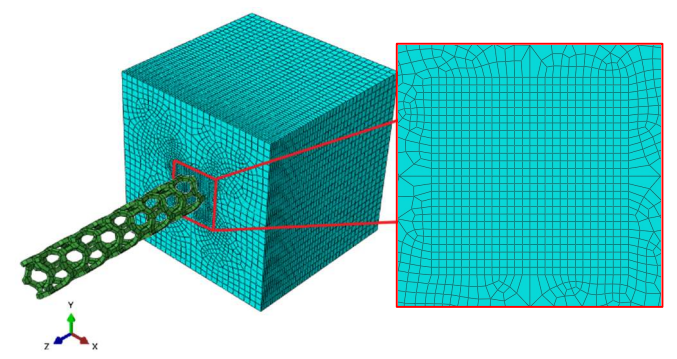


Fig. 2 – Discrete-continuum model of CNT and PEEK polymer substrate

The Lagrangian approach was used for simulating the physical processes, ensuring high calculation accuracy. However, this approach has certain drawbacks, particularly significant mesh distortion in the contact zone during the particle-substrate impact. To minimize these distortions and maintain calculation accuracy, a dynamic failure model was integrated, allowing for the correction of mesh elements and the prevention of excessive deformations by deleting elements that reach the failure criterion

Table 1 – Geometric parameters of CNT model and PEEK substrate

Material	Parameters				
	Lanath nm	Average	Outer/Inner		
	Length, nm	diameter, nm	diameter, nm		
CNT	2.061	0.343	0.383/0.302		
	Length, nm	Width, nm	Thickness, nm		
PEEK	2	2	2		

based on the Johnson-Cook damage model. This method proved more effective than alternatives like ALE adaptive meshing, as it better preserved the physical realism of the deformation process while stabilizing the numerical simulation, according to [10].

The polymer substrate was modeled as a cubic plate with dimensions selected to reduce boundary effects and minimize oscillations generated during dynamic loading. In the simulations, a single-walled carbon nanotube with a (5,0) zigzag configuration consisting of 100 carbon atoms was used. The main geometric parameters of the CNT were determined based on analytical relations [16–18]. The corresponding geometric parameters of the CNT and the substrate are presented in Table 1.

The model included two main factors of the temperature field generation when solving the coupled problem of thermal strength: frictional heating due to the contact of the CNT with the substrate and plastic deformation heating due to the conversion of the kinetic energy of the CNT into thermal energy during substrate deformation. The direction of the impact of the CNT on the polymer substrate was assumed to be perpendicular to the polymer surface. During the impact, both tangential interaction (modeled with a friction coefficient of 0.3) and normal interaction (ensuring "hard" contact conditions with the possibility of a rebound) were taken into account.

The following initial and boundary conditions were set in the calculation scheme: the initial temperatures of the substrate and CNT were 373 K and 296 K, respectively. The CNT velocity was set in the range from 600 m/s to 1000 m/s. The boundary conditions of the substrate along the side and bottom planes corresponded to the symmetry conditions. To avoid possible manifestation of the numerical instability process, the movement of the upper nodes of the finite element model of the CNT was limited in the X and Y directions.

Material Model. Considering the high sensitivity of PEEK to temperature and strain rate, the Johnson-Cook model [19, 20] was used to describe its viscoelastic behavior in this study. Although this model is primarily developed for metals and alloys, it is also applied to polymeric materials, especially when simulating their behavior under conditions of high strain rates and elevated temperatures. Unlike metals, polymers exhibit a pronounced nonlinear

dependence of their mechanical properties on both temperature and strain rate, which makes the use of this model appropriate for simulation purposes. The Johnson-Cook constitutive model is expressed as follows:

$$\sigma\left(\varepsilon_{p},\dot{\varepsilon},T\right) = \left[A + B\varepsilon_{p}^{n}\right]\left[1 + C\ln(\dot{\varepsilon}^{*})\right]\left[1 - \theta^{m}\right],\tag{1}$$

where  $\sigma$  – is the quasi-steady state yield stress, MPa;  $\varepsilon_p$  – is the equivalent plastic strain;  $\dot{\varepsilon}^* = \dot{\varepsilon} / \dot{\varepsilon}_0$  – is the dimensionless plastic strain rate;  $\dot{\varepsilon}$  – is the strain rate, s<sup>-1</sup>;  $\dot{\varepsilon}_0$  – is the reference strain rate, s<sup>-1</sup>;  $\theta = (T - T_r) / (T_m - T_r)$  – is the homologous temperature; T – is the current temperature, K;  $T_r$  – is the reference (initial) temperature, K;  $T_m$  – is the melting temperature, K;  $T_m$  – is the quasi-steady state yield stress, MPa;  $T_m$  – is the power law pre-exponential factor, MPa;  $T_m$  – is the strain rate pre-exponential factor;  $T_m$  – is the strain hardening exponent;  $T_m$  – is the thermal softening exponent.

The temperature gradient during plastic deformation of the polymer was determined based on the formula presented in [13]:

$$\Delta T(\varepsilon_{p}, \dot{\varepsilon}, T) = \frac{\beta}{\rho C_{p}} \int_{\varepsilon}^{\varepsilon_{p}} \sigma(\varepsilon_{p}, \dot{\varepsilon}, T) d\varepsilon_{p}, \qquad (2)$$

where  $\rho$  - is the density, kg/m<sup>3</sup>;  $C_p$  - is the specific heat capacity at constant pressure, J/(kg·K);  $\beta$  - is the Quinney-Taylor heat fraction coefficient.

The Johnson-Cook failure model [17, 18] describes the accumulation of damage and subsequent material failure under conditions of intensive plastic deformation. It takes into account the effects of strain, strain rate, temperature, and hydrostatic pressure.

$$\varepsilon^{f} = \left[ D_{1} + D_{2}e^{D_{3}\frac{p}{q}} \right] \left[ 1 + D_{4}(\ln(\dot{\varepsilon}^{*})) \right] \left[ 1 + D_{5}\theta \right], \tag{3}$$

where  $\varepsilon^f$  is the equivalent plastic strain at damage initiation; p is the pressure, MPa; q is the von Mises stress, MPa;  $D_1 - D_5$  are empirical failure parameters for the material.

Since Young's modulus, Poisson's ratio, and specific heat capacity of PEEK material are strongly temperature-dependent, they were defined as temperature-dependent functions. The data for Young's modulus and Poisson's ratio were adapted from sources [11, 21], whereas the temperature dependence of the specific heat capacity was taken from [22] (Fig. 3-5).

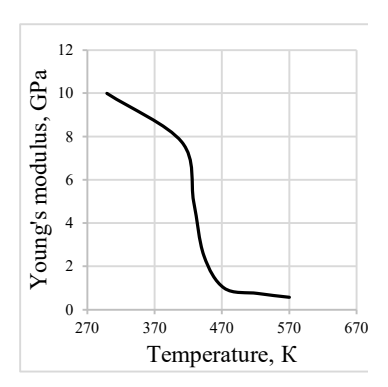


Fig. 3 – Graph of the temperature dependence of Young's modulus for PEEK [11, 21]

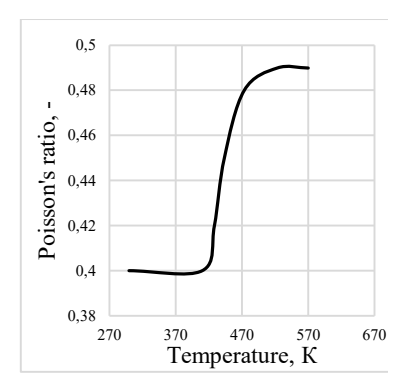


Fig. 4 – Graph of the temperature dependence of Poisson's ratio for PEEK [11, 21]

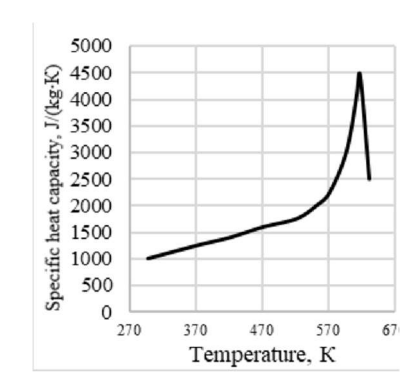


Fig. 5 – Graph of the temperature dependence of specific heat capacity for PEEK [22]

In this study, the equivalent value of Young's modulus between carbon atoms of the nanotube is determined by the stiffness of the C-C covalent bond by analogy with [16, 17, 23]. The mechanical and thermal properties of PEEK and CNT materials are listed in Table 2. The coefficients of the Johnson-Cook plasticity model and the Johnson-Cook failure model for PEEK are listed in Table 3.

Table 2 – Mechanical and thermal properties of materials for PEEK and CNT
---

Properties	Parameters	Unit	Material	
	Parameters		PEEK	CNT
	Density, $\rho$	kg/m <sup>3</sup>	1300	1500
General	Specific heat capacity, $C_p$	J/(kg·K)	$C_p = f(T)$	680
	Thermal conductivity, k	W/(m·K)	0.25	3000
	Thermal expansion coefficient, $\alpha$	10 <sup>-6</sup> /K	140	-
	Quinney-Taylor heat fraction coefficient, $\beta$	-	0.9	-
Elastic	Young's modulus, E	GPa	E=f(T)	6651.4
	Poisson's ratio, v	-	v=f(T)	0

Table 3 – Parameters of the Johnson-Cook plasticity model and Johnson-Cook failure model for PEEK

Properties	Parameters	Unit Value	
Johnson-Cook plasticity model [11]	Quasi-steady state yield stress, A	MPa	132
	Power law pre-exponential factor, B	MPa	32.5
	Strain rate pre-exponential factor, C	-	0.1373
	Thermal softening exponent, m	-	2.01
	Strain hardening exponent, n	-	3.5
	Reference strain rate, $\dot{\varepsilon}_{\scriptscriptstyle 0}$	s <sup>-1</sup>	1.0
	Melting temperature, $T_m$	К	524
	Reference temperature, $T_r$	К	296
Johnson-Cook failure model [24]	1 1		0.05; 1.2; -0.254; -0.09; 1

**Numerical Simulation Results.** To study the conditions of CNT deposition on a polymer plate made of PEEK, a series of numerical experiments was carried out at velocities ranging from 600 to 1000 m/s. Although such velocities are not typical for cold spraying onto polymers, they were used due to the necessity to compensate for the extremely small mass of the nanotube and to ensure sufficient momentum for penetration. At impact velocities below 600 m/s, carbon nanotubes colliding with the substrate simply rebounded from the polymer surface without causing any significant plastic deformation. This behavior is attributed to insufficient kinetic energy, which is inadequate to overcome the resistance of the substrate material. Under these conditions, the impact resulted only in a slight deceleration of the CNT and a change in its trajectory.

To characterize the material behavior under impact loading, four main parameters were used: equivalent plastic strain (PEEQ), temperature (TEMP), von Mises stress (S, Mises), and displacement along the Z-axis (U3).

To analyze the evolution of residual stresses, combined von Mises stress moiré patterns (Fig. 6) were constructed at three key time points:  $0.3 \times 10^{-12}$  s,  $0.5 \times 10^{-12}$  s,  $2 \times 10^{-12}$  s. Each pattern represents a quarter of the contact area between the CNT and the polymer surface, corresponding to different impact velocities: 600, 800, 900, and 1000 m/s. This visualization of the results allows a convenient comparison of the effect of the initial velocity of the CNT on the formation of residual stresses in the polymer matrix.

Though the maximum values of von Mises stress exhibit some randomness due to local deformation features, the general stress distribution pattern allows for a comparative analysis. For this purpose, it is more appropriate to focus on areas of stable residual stresses rather than on peak values. These areas appear as green zones in the visualizations and correspond to intermediate stress levels, serving as a clear marker of the spatial extent of plastic deformation. The analysis shows that as the impact velocity increases, the area of these zones expands significantly, indicating an intensification of residual stress accumulation and deeper penetration of the particle into the substrate material.

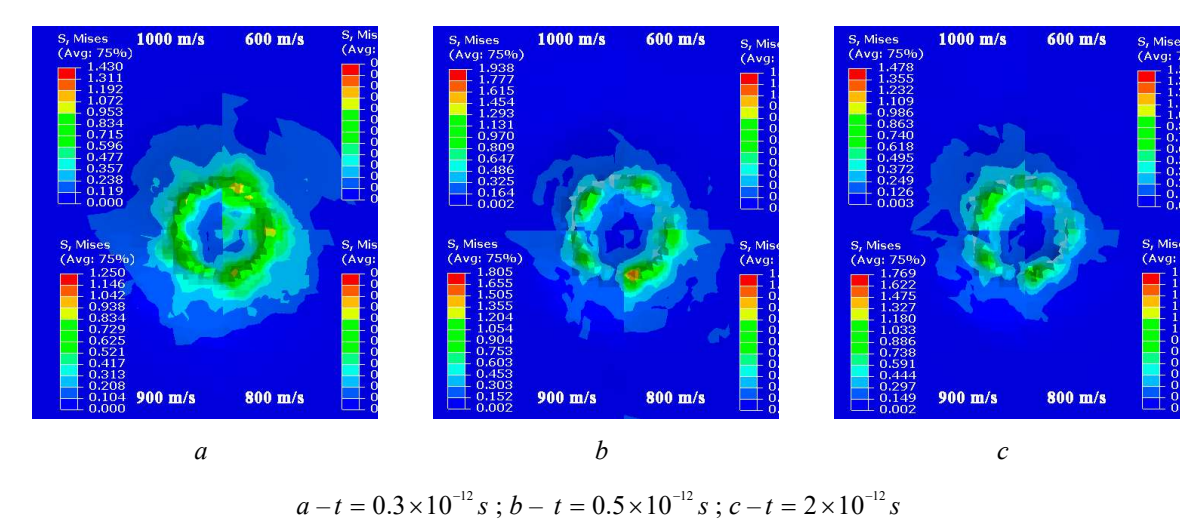


Fig. 6 – Distribution of equivalent von Mises stresses (GPa) depending on the initial velocity of the CNT at representative time intervals of the simulation

Figure 7 shows the spatial temperature distribution as a function of the initial velocity of the carbon nanotube (600 to 1000 m/s) at three representative simulation time intervals.

In all cases, a localized region of elevated temperature forms around the contact area between the nanotube and the substrate. A clear relationship between CNT velocity and temperature rise is observed: at a velocity of 1000 m/s, the temperature in the contact zone reaches 432 K, whereas at 600 m/s it only reaches 393 K.

The temperature rise begins at the direct contact interface between the CNT and the substrate. Subsequently, thermal energy is redistributed towards the central part of the nanotube cavity. This is due to both the geometry of the CNT and the direction of heat flow, which is directed towards areas with lower heat dissipation. The expansion and growth of the heating zone with an increase in impact velocity is a result of the increase in specific energy transferred to the substrate.

After reaching the maximum temperature at the impact zone, there is a sharp drop in temperature due to intense heat dissipation to the peripheral areas of the substrate. Consequently, heat is actively spread from the contact area of the nanotube to the cooler regions of the plate. After the initial peak, the temperature field gradually stabilizes due to the establishment of a local thermal balance between areas with different temperatures and the absence of additional heat sources.

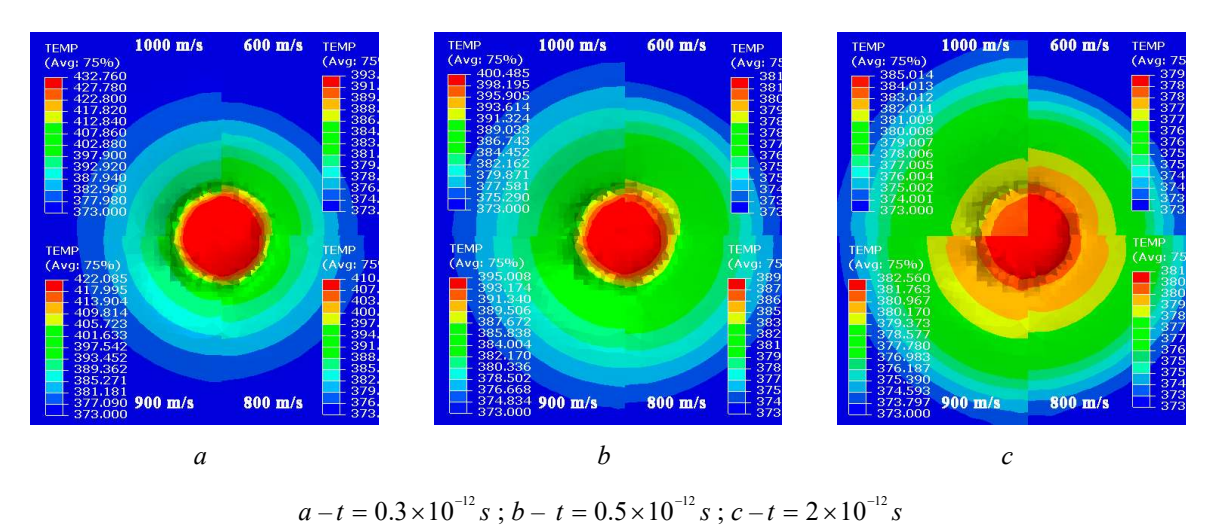


Fig. 7 – Temperature distribution (K) depending on the initial CNT velocity at representative time intervals of the simulation

Figure 8 illustrates that as impact velocity increases, the areas of plastic deformation in the substrate expand both in the contact plane and in depth. Upon impact of the CNT with the PEEK surface, intense localized plastic deformations are generated, accompanied by stress concentration and active heat release due to internal friction and energy dissipation.

As plastic strain accumulates, the material stiffness decreases, resulting in softening of the contact zone. This softening causes the deformed substrate material to be displaced laterally from the impact axis, forming a characteristic symmetrical (circular) deformation pattern around the CNT.

When impact velocities increase, the depth of nanotube penetration into the substrate increases significantly. This increase is caused by the higher kinetic energy of the CNT and the elevated level of plastic deformation in the polymer at the contact area.

Figure 9 shows the evolution of changes in the basic physical parameters in the contact area between the CNT and the PEEK polymer substrate as a function of the initial impact velocities (600 to 1000 m/s): depth of penetration, temperature, equivalent von Mises stress, plastic strain, and accumulated defects.

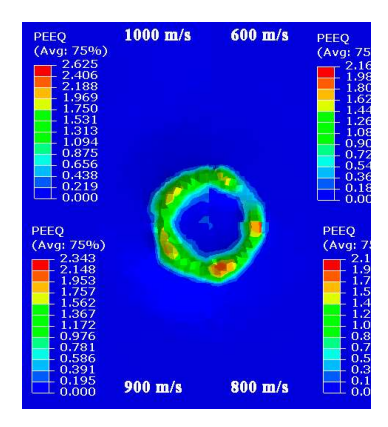
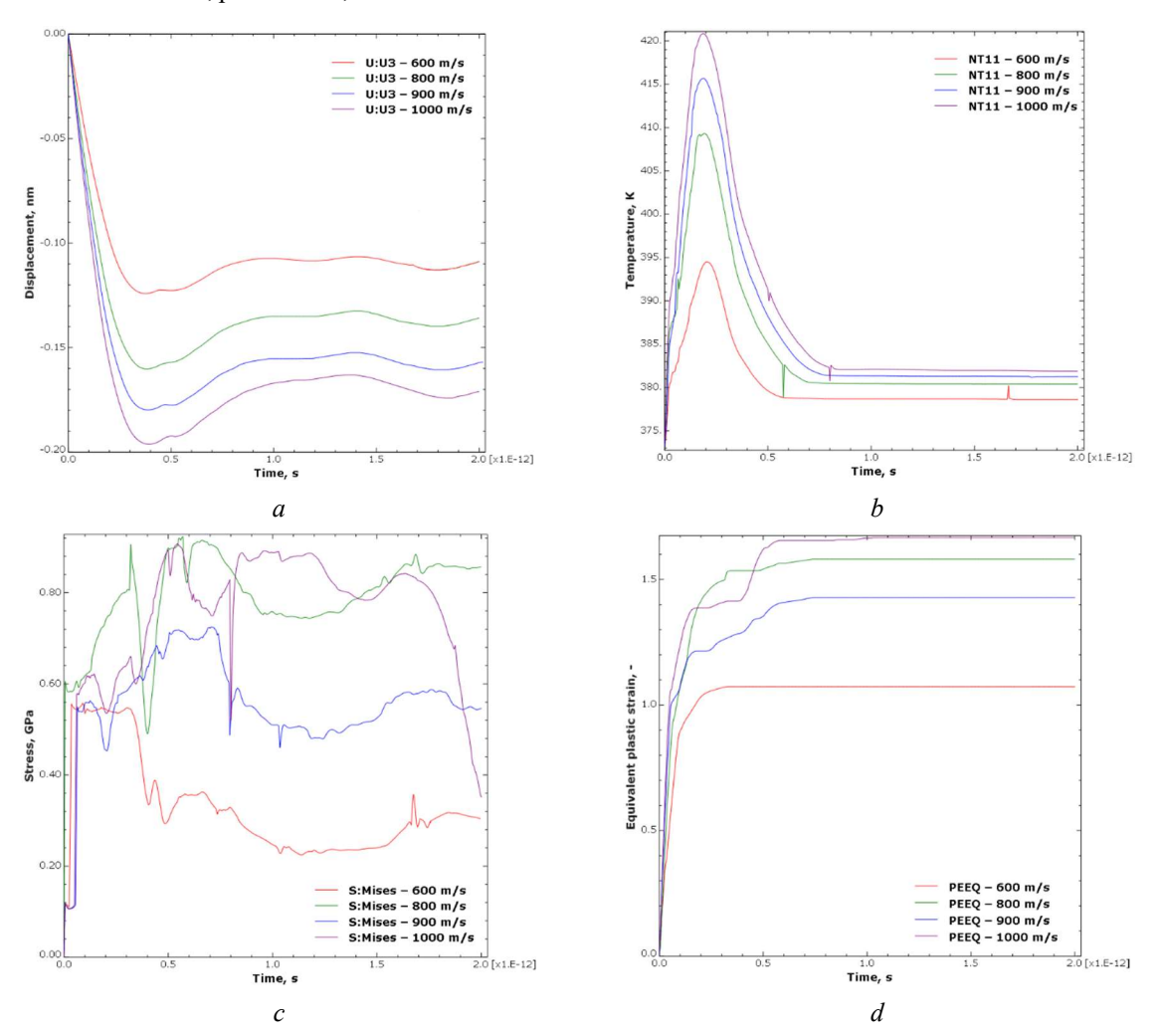


Fig. 8 – Distribution of equivalent plastic strain depending on the initial CNT velocity



a – penetration depth; b – temperature; c – von Mises stresses; d – equivalent plastic strain
 Fig. 9 – Time evolution of the contact interaction parameters between CNT and substrate depending on different initial nanotube velocities

The plot (Fig. 9, a) shows the dependence of vertical displacement (U3) of the nanotube on time at various initial velocities (600 to 1000 m/s). As the impact velocity increases, the depth of CNT penetration into the substrate increases from 0.10 nm at 600 m/s to 0.19 nm at 1000 m/s. his parameter rapidly reaches its maximum during the first  $0.3 \times 10^{-12}$  s and then decreases, entering a damping oscillatory regime. The further partial recovery is related to the plastic properties of the substrate material.

It should be noted that the maximum temperature (Fig. 9, b) in the contact area abruptly rises to 397 K at 600 m/s and 425 K at 1000 m/s in all deformation modes, and the temperature value is proportional to the velocity of the nanotube. This effect can be explained by the higher intensity of localized plastic deformation. After reaching the maximum temperature, the temperature sharply decreases due to the thermal conductivity of the substrate material and heat dissipation into the bulk of the polymer. After this, the temperature in the time interval under study ( $2 \times 10^{-12}$  s) stabilizes between 378 K and 385 K.

The evolution of equivalent stresses according to von Mises stress (Fig. 9, c) exhibits complex and unstable behavior. At higher impact velocities, these stresses are characterized by higher amplitudes and more frequent fluctuations, indicating the occurrence of intense oscillatory processes in the substrate material. The stresses reach their peak values shortly after impact, after which they decrease and stabilize at a level that also correlates with the impact velocity.

The plot of equivalent plastic strain (Fig. 9, d) confirms the characteristic accumulation of residual plastic strains. The highest values, exceeding 1.7, are observed at 1000 m/s, indicating significant plastic deformation in the contact area and the initiation of fracture.

The results of the numerical simulation have shown that effective deposition of the carbon nanotube on the surface of the polyetheretherketone polymer substrate is achieved at an impact velocity of 1000 m/s (Fig. 10).

Thus, the primary mechanism for stable anchoring of the CNT is localized compaction and partial penetration of the nanotube into the substrate due to the combined action of several physical factors.

Firstly, at a velocity of 1000 m/s, the maximum penetration depth of the CNT reaches 0.19 nm, ensuring its partial embedding into the polymer surface layer. Secondly, the impact is accompanied by a local temperature rise up to 432 K in the contact area, which exceeds the glass transition temperature of PEEK (400 K). Under such conditions, the polymer transitions into a rubbery, highly elastic state characterized by a significant decrease in mechanical stiffness and increased susceptibility to plastic deformation. This allows the polymer to deform around the nanotube, partially interlocking it.

Additionally, local thermal expansion of the material in the impact area further enhances the effect of mechanical entrapment of the nanotube within the polymer plate. After impact, rapid cooling of the system occurs, lowering the temperature below the glass transition point due to the thermal conductivity of the substrate. As a result, the PEEK substrate restores its original stiffness and rigidity, securely fixing the CNT within the solidified structure.

Thus, the mechanism of CNT adhesion to the polymer substrate is achieved through the combined effect of three key factors: sufficient penetration depth, temporary softening of the polymer due to localized temperature increase, and subsequent restoration of rigidity upon cooling. The interaction of these effects ensures reliable mechanical fixation of the nanotubes in the substrate.

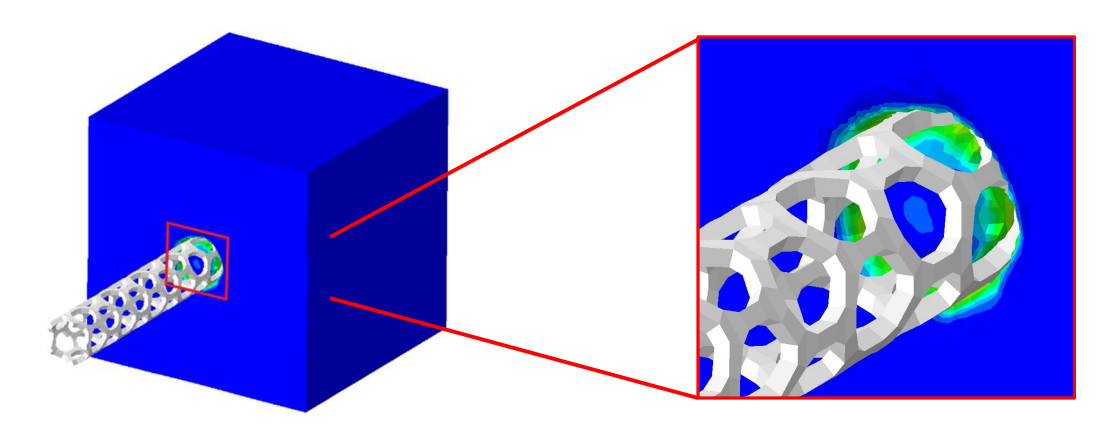


Fig. 10 – The image of the CNT fixed in the PEEK polymer matrix due to impact interaction at a velocity of 1000 m/s

**Conclusion.** Within the framework of this study, the process of cold spraying of carbon nanotubes onto a polymer substrate made of polyetheretherketone has been investigated numerically. The study has provided a detailed analysis of the effects of impact velocity on the ability to achieve CNT fixation within the polymer substrate.

The simulation results revealed that at velocities below 600 m/s, the mechanical impulse of the CNT particles is insufficient to overcome the resistance of the substrate, resulting in particle rebound without the formation of a stable bond with the surface.

As the impact velocity increases, the intensity of plastic deformation and thermal effects in the contact area also rises gradually. However, only at a velocity of 1000 m/s is a favorable environment for CNT fixation achieved. Under these specific conditions, the combined action of three critically important factors occurs: deep penetration of the particles into the material, temperature exceeding the glass transition point of PEEK leading to a temporary decrease in polymer rigidity, and subsequent cooling that locks the nanotubes within the deformed polymer structure.

It has been established that the effective fixation of CNT in the polymer substrate results from localized thermal-structural effects induced by high impact velocities.

This study presents the results of collaborative research conducted by the National Technical University of Ukraine "Igor Sikorsky Kyiv Polytechnic Institute" and the University of Kaiserslautern-Landau, Kaiserslautern (Germany) within the framework of the Leonhard Euler grant program administered by DAAD.

**Further research prospects.** The current study considered only normal (perpendicular) collisions between particles and the substrate surface. However, under practical conditions, the impact angle often deviates from the normal, which can substantially alter the deformation behavior and thermal effects in the contact area. Therefore, future research will focus on analyzing the effect of the CNT impact angle on the efficiency of nanotube fixation within the polymer substrate during the cold spraying process.

#### References

- 1. Champagne V. The Cold Spray Materials Deposition Process: Fundamentals and Applications. Series in Metals and Surface Engineering Series Woodhead Publishing Limited, 2007. ISBN: 978-1-84569-181-3
- 2. Shah, S., Lee, J., Rothstein, J. P. (2017). Numerical Simulations of the High-Velocity Impact of a Single Polymer Particle During Cold-Spray Deposition. *Journal of Thermal Spray Technology*. **26**. P. 970–984. https://doi.org/10.1007/s11666-017-0557-2
- 3. Jing Xie. Simulation of cold spray particle deposition process. Mechanics of materials [physics.class-ph]. INSA de Lyon, 2014. URL: https://theses.hal.science/tel-01153225v1 (Accessed: 15.03.2025)
- 4. Papyrin A., Kosarev V., Klinkov S., et al. Cold Spray Technology. Amsterdam. Elsevier Science, 2006. 336 p. ISBN: 9780080451558
- 5. Wang, X., Feng, F., Klecka, M. A., et al. (2015). Characterization and modeling of the bonding process in cold spray additive manufacturing. *Additive Manufacturing*. **8**. P. 149–162. <a href="https://doi.org/10.1016/j.addma.2015.03.006">https://doi.org/10.1016/j.addma.2015.03.006</a>
- 6. Watanabe, Y., Yoshida, C., Atsumi, K., et al. (2014). Influence of Substrate Temperature on Adhesion Strength of Cold-Sprayed Coatings. *Journal of Thermal Spray Technology*. **24**. P. 86–91. <a href="https://doi.org/10.1007/s11666-014-0165-3">https://doi.org/10.1007/s11666-014-0165-3</a>
- 7. Tan, A., Lek, J., Sun, W., et al. (2018). Influence of Particle Velocity When Propelled Using N2 or N2-He Mixed Gas on the Properties of Cold-Sprayed Ti6Al4V Coatings. *Coatings*. **8** (9). P. 327. https://doi.org/10.3390/coatings8090327
- 8. Chu, X., Che, H., Vo, P., et al. (2017). Understanding the cold spray deposition efficiencies of 316L/Fe mixed powders by performing splat tests onto as-polished coatings. *Surface and Coatings Technology*. **324**, P. 353–360. <a href="https://doi.org/10.1016/j.surfcoat.2017.05.083">https://doi.org/10.1016/j.surfcoat.2017.05.083</a>
- 9. Assadi, H., Gärtner, F., Stoltenhoff, T. et al. (2003). Bonding mechanism in cold gas spraying. *Acta Materialia*. **51** (15), P. 4379–4394. <a href="https://doi.org/10.1016/s1359-6454(03)00274-x">https://doi.org/10.1016/s1359-6454(03)00274-x</a>
- 10. Li, W.-Y., Gao, W. (2009). Some aspects on 3D numerical modeling of high velocity impact of particles in cold spraying by explicit finite element analysis. *Applied Surface Science*. **255** (18), P. 7878–7892. <a href="https://doi.org/10.1016/j.apsusc.2009.04.135">https://doi.org/10.1016/j.apsusc.2009.04.135</a>
- 11. Heydari Astaraee, A., Colombo, C., Bagherifard, S. (2022). Insights on metallic particle bonding to thermoplastic polymeric substrates during cold spray. *Scientific Reports.* **12** (118123). <a href="https://doi.org/10.1038/s41598-022-22200-5">https://doi.org/10.1038/s41598-022-22200-5</a>

- 12. Heydari Astaraee, A., Colombo, C., Bagherifard, S. (2021). Numerical Modeling of Bond Formation in Polymer Surface Metallization Using Cold Spray. *Journal of Thermal Spray Technology*. **30**. P. 1765–1776. <a href="https://doi.org/10.1007/s11666-021-01224-9">https://doi.org/10.1007/s11666-021-01224-9</a>
- 13. Tang, W., Zhang, J., Li, Y., et al. (2021). Numerical Simulation of the Cold Spray Deposition of Copper Particles on Polyether Ether Ketone (PEEK) Substrate. *Journal of Thermal Spray Technology*. **30**. P. 1792–1809. <a href="https://doi.org/10.1007/s11666-021-01254-3">https://doi.org/10.1007/s11666-021-01254-3</a>
- 14. Ata, N., Ohtake, N., Akasaka, H., (2017). Polyethylene–Carbon Nanotube Composite Film Deposited by Cold Spray Technique. *Journal of Thermal Spray Technology*. **26** (7), P. 1541–1547. <a href="https://doi.org/10.1007/s11666-017-0617-7">https://doi.org/10.1007/s11666-017-0617-7</a>
- 15. Ata, N., Okimura, N., Ohtake, N., et al. (2019). Aligned Carbon Nanotube-polymer Composite Film Deposited by a Low-pressure Cold Spray Process. *Seikei-Kakou*. **31** (2), P. 85–89. https://doi.org/10.4325/seikeikakou.31.85
- 16. Scarpa F., Adhikari S. (2008). A mechanical equivalence for Poisson's ratio and thickness of C–C bonds in single wall carbon nanotubes. *Journal of Physics D: Applied Physics.* **41**, 085306. <a href="https://doi.org/10.1088/0022-3727/41/8/085306">https://doi.org/10.1088/0022-3727/41/8/085306</a>
- 17. Gondlyakh, A. V., Sokolskiy, A. L., Kolosov, A. E. et al. (2020). Modeling the Mechanisms of Fracture Formation in Nanomodified Polymers. 2020 IEEE 10th International Conference Nanomaterials: Applications & Properties (NAP), Sumy, Ukraine. https://doi.org/10.1109/nap51477.2020.9309637
- 18. Gondliakh O., Mamchur O. (2022). Parameters of crack resistance of nanoreinforced polymeric engineering products. *Proceedings of the NTUU "Igor Sikorsky KPI"*. Series: Chemical engineering, ecology and resource saving. 4. P. 9–20. https://doi.org/10.20535/2617-9741.4.2022.269740
- 19. Johnson G.R., Cook W.H. (1983). A constitutive model and data for metals subjected to large strains, high strain rates, and high temperatures. *Proceedings of the 7th International Symposium on Ballistics*. P. 541–547. URL: <a href="https://ia800406.us.archive.org/4/items/AConstitutiveModelAndDataForMetals/A%20constitutive%20model%20and%20data%20for%20metals\_text.pdf">https://ia800406.us.archive.org/4/items/AConstitutiveModelAndDataForMetals/A%20constitutive%20model%20and%20data%20for%20metals\_text.pdf</a> (Accessed: 15.03.2025)
- 20. Johnson G. R., Cook W. H. (1985). Fracture Characteristics of Three Metals Subjected to Various Strains, Strain Rates, Temperatures and Pressures. *Engineering Fracture Mechanics*. **21** (1), P. 31-48. http://dx.doi.org/10.1016/0013-7944(85)90052-9
- 21. Maksimov R. D., Kubat J. (1997). Time and temperature dependent deformation of poly(ether ether ketone) (PEEK). *Mechanics of Composite Materials*. **33** (6), P. 517–525. <a href="https://doi.org/10.1007/bf02269611">https://doi.org/10.1007/bf02269611</a>
- 22. Koerdt, M., Koerdt, M., Grobrüg, T., et al. (2019). Modelling and analysis of the thermal characteristic of thermoplastic composites from hybrid textiles during compression moulding. *Journal of Thermoplastic Composite Materials*. **35** (1), P. 127–146. <a href="https://doi.org/10.1177/0892705719875204">https://doi.org/10.1177/0892705719875204</a>
- 23. Yakobson B. I., Brabec C. J., Bernholc J. (1996). Nanomechanics of Carbon Tubes: Instabilities beyond Linear Response. *Physical Review Letters*. **76** (14), P. 2511–2514. <a href="https://doi.org/10.1103/physrevlett.76.2511">https://doi.org/10.1103/physrevlett.76.2511</a>
- 24. Garcia-Gonzalez D. et al. (2015) Mechanical impact behavior of polyether-ether-ketone (PEEK). *Composite Structures*. **124**, P. 88–99. URL: <a href="https://doi.org/10.1016/j.compstruct.2014.12.061">https://doi.org/10.1016/j.compstruct.2014.12.061</a>

# Гондлях О. В., Янковський І. О., Антонюк С. І.

# ОСОБЛИВОСТІ НАНЕСЕННЯ ВУГЛЕЦЕВИХ НАНОТРУБОК НА ПОЛІМЕРНУ ОСНОВУ МЕТОДОМ ХОЛОДНОГО ГАЗОДИНАМІЧНОГО НАПИЛЕННЯ

Холодне газодинамічне напилення вуглецевих нанотрубок на полімерні матеріали у якості підкладки є перспективним методом формування функціональних покриттів, але процес осадження частинок на полімерних основах залишається недостатньо вивченим. У даній роботі розроблено чисельну модель для аналізу механізмів контактної взаємодії вуглецевих нанотрубок із поліефірефіркетоновою (ПЕЕК) підкладкою під час напилення при швидкостях 600 — 1000 м/с. Чисельне моделювання проведено в програмному забезпечені ABAQUS/Explicit з використанням методу скінченних елементів. Враховано модель пластичності Джонсона-Кука та модель руйнування Джонсона-Кука. Досліджено вплив швидкості на процеси пластичної деформації, локального нагрівання та умови закріплення нанотрубок на поверхні

полімерної основи. При ударних швидкостях, менших за 600 м/с, ВНТ при зіткненні з підкладкою лише відскакує від поверхні полімеру, не спричиняючи суттєвих пластичних деформацій. Зі збільшенням швидкості удару зони пластичної деформації в підкладці розширюються як у площині контакту, так і в глибину. При зіткненні ВНТ з поверхнею ПЕЕК виникає інтенсивна локалізована пластична деформація, що супроводжується зосередженням напружень та активним тепловиділенням у результаті внутрішнього тертя та дисипації енергії. За рахунок збільшення швидкості удару глибина проникнення ВНТ у підкладку зростає: від 0,10 нм при 600 м/с до 0,19 нм при 1000 м/с. Температура в зоні контакту різко зростає до 397 К при 600 м/с і до 432 К при 1000 м/с, її величина пропорційна швидкості нанотрубки. Це пояснюється вищою інтенсивністю локалізованої пластичної деформації. Після піку температура стрімко зменшується внаслідок теплопровідності матеріалу підкладки та розподілу тепла вглиб масиву полімеру. Ефективна фіксація вуглецевої нанотрубки на поверхні полімерної підкладки з поліефірефіркетону досягається за умови ударної швидкості 1000 м/с. При швидкості 1000 м/с спостерігається максимальна глибина проникнення ВНТ до 0,19 нм, що забезпечує її часткове занурення в поверхневий шар полімеру. Удар супроводжується локальним підвищенням температури в зоні контакту до 432 К, що перевищує температуру склування ПЕЕК (400 К). За таких умовах полімер переходить у високоеластичний стан, що супроводжується значним зниженням механічної жорсткості та підвищенням податливості до пластичної деформації. Це дає змогу полімеру деформуватися навколо нанотрубки, частково її охоплюючи. Локальне термічне розширення матеріалу в зоні удару додатково посилює ефект механічного захоплення нанотрубки в полімерній пластині. Після завершення ударної взаємодії відбувається швидке охолодження системи до температури нижче точки склування, зумовлене теплопровідністю підкладки. В результаті ПЕЕК відновлює свої вихідні жорсткі властивості, фіксуючи ВНТ у застиглій структурі. Критична швидкість 1000 м/с забезпечує надійну фіксацію ВНТ у ПЕЕК завдяки локальним термо-структурним ефектам. Запропонована модель дозволяє прогнозувати оптимальні параметри процесу напилення для забезпечення високої ефективності напилення нанотрубок.

**Ключові слова**: холодне газодинамічне напилення, вуглецеві нанотрубки, поліефірефіркетон, метод скінченних елементів

## Список використаної літератури

- 1. The Cold Spray Materials Deposition Process: Fundamentals and applications / ed. by V. K. Champagne. Cambridge: Elsevier Science, 2007. 376 p. ISBN: 978-1-84569-181-3
- 2. Shah S., Lee J., Rothstein J. P. Numerical Simulations of the High-Velocity Impact of a Single Polymer Particle During Cold-Spray Deposition. *Journal of Thermal Spray Technology*. 2017. Vol. 26. P. 970–984. https://doi.org/10.1007/s11666-017-0557-2
- 3. Jing Xie. Simulation of cold spray particle deposition process. Mechanics of materials [physics.class-ph]. INSA de Lyon, 2014. URL: <a href="https://theses.hal.science/tel-01153225v1">https://theses.hal.science/tel-01153225v1</a> (дата звернення: 15.03.2025).
- 4. Cold Spray Technology / A. Papyrin et al. Amsterdam: Elsevier Science, 2006. 336 p. ISBN: 9780080451558
- 5. Characterization and modeling of the bonding process in cold spray additive manufacturing / X. Wang et al. *Additive Manufacturing*. 2015. Vol. 8. P. 149–162. <a href="https://doi.org/10.1016/j.addma.2015.03.006">https://doi.org/10.1016/j.addma.2015.03.006</a>
- 6. Influence of Substrate Temperature on Adhesion Strength of Cold-Sprayed Coatings / Y. Watanabe et al. *Journal of Thermal Spray Technology*. 2014. Vol. 24. P. 86–91. <a href="https://doi.org/10.1007/s11666-014-0165-3">https://doi.org/10.1007/s11666-014-0165-3</a>
- 7. Influence of Particle Velocity When Propelled Using N2 or N2-He Mixed Gas on the Properties of Cold-Sprayed Ti6Al4V Coatings / A. W.-Y. Tan et al. *Coatings*. 2018. Vol. 8, Issue 9. P. 327. https://doi.org/10.3390/coatings8090327
- 8. Understanding the cold spray deposition efficiencies of 316L/Fe mixed powders by performing splat tests onto as-polished coatings / X. Chu et al. *Surface and Coatings Technology*. 2017. Vol. 324. P. 353–360. https://doi.org/10.1016/j.surfcoat.2017.05.083
- 9. Bonding mechanism in cold gas spraying / H. Assadi et al. *Acta Materialia*. 2003. Vol. 51, Issue 15. P. 4379– 4394. <a href="https://doi.org/10.1016/s1359-6454(03)00274-x">https://doi.org/10.1016/s1359-6454(03)00274-x</a>
- 10. Li W.-Y., Gao W. Some aspects on 3D numerical modeling of high velocity impact of particles in cold spraying by explicit finite element analysis. *Applied Surface Science*. 2009. Vol. 255, Issue 18. P. 7878–7892. https://doi.org/10.1016/j.apsusc.2009.04.135

- 11. Heydari Astaraee A., Colombo C., Bagherifard S. Insights on metallic particle bonding to thermoplastic polymeric substrates during cold spray. *Scientific Reports*. 2022. Vol. 12, Article Number 18123. https://doi.org/10.1038/s41598-022-22200-5
- 12. Heydari Astaraee A., Colombo C., Bagherifard S. Numerical Modeling of Bond Formation in Polymer Surface Metallization Using Cold Spray. *Journal of Thermal Spray Technology*. 2021. Vol. 30. P. 1765–1776. https://doi.org/10.1007/s11666-021-01224-9
- 13. Numerical Simulation of the Cold Spray Deposition of Copper Particles on Polyether Ether Ketone (PEEK) Substrate / W. Tang et al. *Journal of Thermal Spray Technology*. 2021. Vol. 30. P. 1792–1809. https://doi.org/10.1007/s11666-021-01254-3
- 14. Ata N., Ohtake N., Akasaka H. Polyethylene–Carbon Nanotube Composite Film Deposited by Cold Spray Technique. *Journal of Thermal Spray Technology*. 2017. Vol. 26. P. 1541–1547. <a href="https://doi.org/10.1007/s11666-017-0617-7">https://doi.org/10.1007/s11666-017-0617-7</a>
- 15. Aligned Carbon Nanotube-polymer Composite Film Deposited by a Low-pressure Cold Spray Process / N. Ata et al. *Seikei-Kakou*. 2019. Vol. 31, Issue 2. P. 85–89. <a href="https://doi.org/10.4325/seikeikakou.31.85">https://doi.org/10.4325/seikeikakou.31.85</a>
- 16. Scarpa F., Adhikari S. A mechanical equivalence for Poisson's ratio and thickness of C–C bonds in single wall carbon nanotubes. *Journal of Physics D: Applied Physics*. 2008. Vol. 41, Issue. 8. P. 085306. https://doi.org/10.1088/0022-3727/41/8/085306
- 17. Modeling the Mechanisms of Fracture Formation in Nanomodified Polymers / A. Gondlyakh, A. Sokolskiy, T. Shylovych, Ya. Shylovych, A. Chemeris, S. Antonyuk. 2020 IEEE 10th International Conference Nanomaterials: Applications & Properties (NAP), Sumy, Ukraine, 9–13 November 2020. https://doi.org/10.1109/nap51477.2020.9309637
- 18. Gondliakh O., Mamchur O. Parameters of crack resistance of nanoreinforced polymeric engineering products. *Proceedings of the NTUU "Igor Sikorsky KPI"*. Series: Chemical engineering, ecology and resource saving. 2022. № 4. C. 9–20. URL: https://doi.org/10.20535/2617-9741.4.2022.269740
- 19. Johnson G. R., Cook W.H. A constitutive model and data for metals subjected to large strains, high strain rates, and high temperatures. *Proceedings of the 7th International Symposium on Ballistics*. The Hague. 1983. P. 541–547.

  URL: <a href="https://ia800406.us.archive.org/4/items/AConstitutiveModelAndDataForMetals/A%20constitutive%20model%20and%20data%20for%20metals\_text.pdf">https://ia800406.us.archive.org/4/items/AConstitutiveModelAndDataForMetals/A%20constitutive%20model%20and%20data%20for%20metals\_text.pdf</a> (дата звернення: 15.03.2025).
- 20. Johnson G. R., Cook W. H. Fracture Characteristics of Three Metals Subjected to Various Strains, Strain Rates, Temperatures and Pressures. *Engineering Fracture Mechanics*. 1985. Vol. 21, Issue 1. P. 31-48. <a href="http://dx.doi.org/10.1016/0013-7944(85)90052-9">http://dx.doi.org/10.1016/0013-7944(85)90052-9</a>
- 21. Maksimov R. D., Kubat J. Time and temperature dependent deformation of poly(ether ether ketone) (PEEK). *Mechanics of Composite Materials*. 1997. Vol. 33, Issue 6. P. 517–525. https://doi.org/10.1007/bf02269611
- 22. Modelling and analysis of the thermal characteristic of thermoplastic composites from hybrid textiles during compression moulding / M. Koerdt et al. *Journal of Thermoplastic Composite Materials*. 2019. Vol. 35, Issue 1. P. 127-146. https://doi.org/10.1177/0892705719875204
- 23. Yakobson B. I., Brabec C. J., Bernholc J. Nanomechanics of Carbon Tubes: Instabilities beyond Linear Response. *Physical Review Letters*. 1996. Vol. 76, Issue 14. P. 2511–2514. <a href="https://doi.org/10.1103/physrevlett.76.2511">https://doi.org/10.1103/physrevlett.76.2511</a>
- 24. Mechanical impact behavior of polyether–ether–ketone (PEEK) / D. Garcia-Gonzalez et al. *Composite Structures*. 2015. Vol. 124. P. 88–99. URL: <a href="https://doi.org/10.1016/j.compstruct.2014.12.061">https://doi.org/10.1016/j.compstruct.2014.12.061</a>